

Determination of optimal laser power according to the tool path inclination angle of a titanium alloy workpiece in laser-assisted machining

Min Seop Sim¹ · Choon Man Lee¹

Received: 22 March 2015 / Accepted: 3 August 2015 / Published online: 18 August 2015
© Springer-Verlag London 2015

Abstract The purpose of this work was to study laser-assisted machining (LAM) according to the tool path inclination angle of a titanium alloy workpiece. Previous studies have investigated using LAM for the linear machining of difficult-to-cut materials. However, during the linear machining of an inclined planar workpiece, the laser spot is deformed into an elliptical shape, and then, the tool follows the long major axis of the elliptical laser spot. For tool path inclination angle machining, the tool follows the arbitrarily oriented direction of the elliptical laser spot. Thus, determining the preheating temperature of the workpiece by tool path inclination angle processing is different from that of linear processing. In this work, a study was carried out to optimize the preheating and machining based on the tool path inclination angle. The optimal laser power according to tool path inclination angle was determined through thermal analysis, and the thermal analysis results were compared with the results from preheating experiments. Also, machining experiments were conducted using the as-determined laser power.

Keywords Laser-assisted machining · Finite element method · Tool path inclination angle · Titanium alloy · Cutting force

1 Introduction

With recent advances in machining technologies, studies are being actively conducted to find ways of machining materials that have been difficult to process in the past [1–4]. Materials that have been difficult to process include fine ceramics, superalloys, titanium, and nickel-based alloys [5]. Such materials are difficult to machine due to their high levels of brittleness, durability, and thermal resistance, and that limits their commercial uses, because of corresponding high machining costs [6, 7]. Among other methods, laser-assisted machining (LAM) has been widely studied as a technology for machining such difficult-to-cut materials [8, 9]. This machining method processes a specific area after it has been softened by laser-based preheating. It has been highlighted as an effective method because it allows smooth machining by increasing the ductility of the materials, while inhibiting brittleness [10, 11]. LAM enables easy machining of not only ceramics but also other materials, such as nickel-based alloys, including Inconel 718, Nickel 201, and so on, as well as titanium alloys. Thus, it is considered an excellent machining method because it can greatly reduce machining expenses. Following recent global trends, however, studies on this machining method have largely been limited to turning processes. In contrast to turning, milling is still carried out at the level of machining one-dimensional flat materials. To evaluate the practical issues involved in milling, which can advance its use for machining a greater variety of shapes, studies on laser-assisted milling (LAMill) are required. In response to this need, many studies on the machining of materials in various shapes using laser-assisted milling have been conducted throughout the world. However, one of the difficulties of using this method is that it requires estimating a moving heat source over complex shaped materials. Additional precise analyses and studies are also required because the shapes of the heat sources vary [12, 13].

✉ Choon Man Lee
cmlee@changwon.ac.kr

¹ School of Mechanical Engineering, Changwon National University, #9 Sarim-dong, Changwon-si, Gyeongsangnam-do 641-773, Republic of Korea

Kaylon et al. [14] calculated the surface temperatures of materials according to changes in time using numerical analysis when the materials were preheated in a LAM process. Yang et al. [15] investigated the interactive mechanism between a laser and silicon nitride in a LAM process with a silicon nitride material. Kim et al. [16] proposed a new laser heat source projection method for the analysis of square and spline members and predicted the temperature distribution of the members based on their rotation. Kim et al. [17] studied the machining parameters of nickel-based alloys using a high-power diode laser in order to improve the surface quality. Rozzi et al. [18] performed a study estimating the surface temperature of silicon nitride using numerical analysis in LAM. Kim et al. [19] investigated the preheating temperature and cutting force of AISI 1045 and Inconel 718 using an experimental design method. Kang et al. [20, 21] performed silicon nitride and AISI 1045 steel machining using LAM and determined coefficients in constitutive equations using the cutting force obtained in this process. Lei et al. [22] applied a two-dimensional shear angle model to determine shear angles in a silicon nitride LAM process. Also, they proposed a constitutive equation for presenting a deformation structure by analyzing shear stresses based on a three-dimensional theory and an experimental study.

In this work, a study on LAM based on the tool path inclination angle was carried out. The cutting force of the tool path inclination angle of titanium alloy with a rotated angle for one axis was measured during preheating and machining [23].

2 Finite element model

2.1 Governing equation

The three-dimensional transient analysis by temperature-dependent inputs is described by Eq. (1) [19] as

$$\alpha \left(\frac{\partial^2 T}{\partial x^2} + \frac{\partial^2 T}{\partial y^2} + \frac{\partial^2 T}{\partial z^2} \right) + \dot{Q} = \frac{\partial T}{\partial t}, \quad \alpha = \frac{k}{\rho C_p} \quad (1)$$

where T , ρ , C_p , k , t , α , and \dot{Q} represent temperature, density, specific heat, thermal conductivity, time, thermal expansion coefficient, and power generation per unit volume, respectively.

The initial condition at time $t=0$ is given by Eq. (2) as follows:

$$T(x, y, z, 0) = T_0 \quad (2)$$

The boundary conditions can be defined by Eq. (3) as

$$-k \frac{\partial T}{\partial z} = q(x, y) - h(T - T_0) \quad (3)$$

where q , h , T , and T_0 are the heat flux, heat transfer coefficient, surface temperature, and ambient temperature, respectively.

2.2 Method of heat source modeling

In a LAM process, it is very important to estimate the preheating temperatures of materials and to maintain proper machining temperatures, by controlling laser power according to changes in feed rates [19]. In this study, to estimate preheating temperatures, thermal analysis was performed using the ANSYS Workbench, which is a finite element analysis software program. It is not easy to represent a moving laser heat source since it does not remain at a fixed point, and it is difficult to describe it in steady-state analysis using finite element analysis. To represent a moving heat source, circles of heat sources are moved by a half circle for a half-circle overlapped model. As shown in Fig. 1, in this study, the circle was moved by 1.5 mm because the diameter of the laser heat source used was 3 mm [23, 24].

2.3 Analysis model

The analysis model used in the finite element analysis for the tool path inclination angle is presented in Fig. 2. There are two types of inclination angles. The first type depends on the inclination in the workpiece itself as shown in Fig. 2a. The rotated angles with respect to one axis are given by 0° , 15° , 30° , 45° , and 60° . The second type is determined by the tool path inclination angles, as shown in Fig. 2b, which were set as 0° , 15° , 30° , 45° , 60° , 75° , and 90° .

Figure 3 shows the mesh used in the analysis. A hexagonal mesh was applied in the analysis model which included 85,392 nodes and 24,841 elements. The mesh sizes of the jig, inclination face, and laser heating zone used were 3, 1, and 0.25 mm, respectively.

2.4 Determination of laser absorptivity

The laser absorptivity of titanium alloy is approximately 0.35–0.4 [25, 26]. Kim et al. [25] suggested an equation on the absorptivity of a diode laser for titanium alloy as follows:

$$A = \frac{m \cdot c_p \cdot \Delta T}{E_l \cdot \Delta t} \quad (4)$$

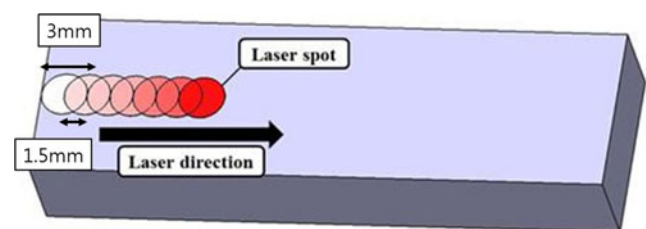


Fig. 1 Sequential moving method of heat sources

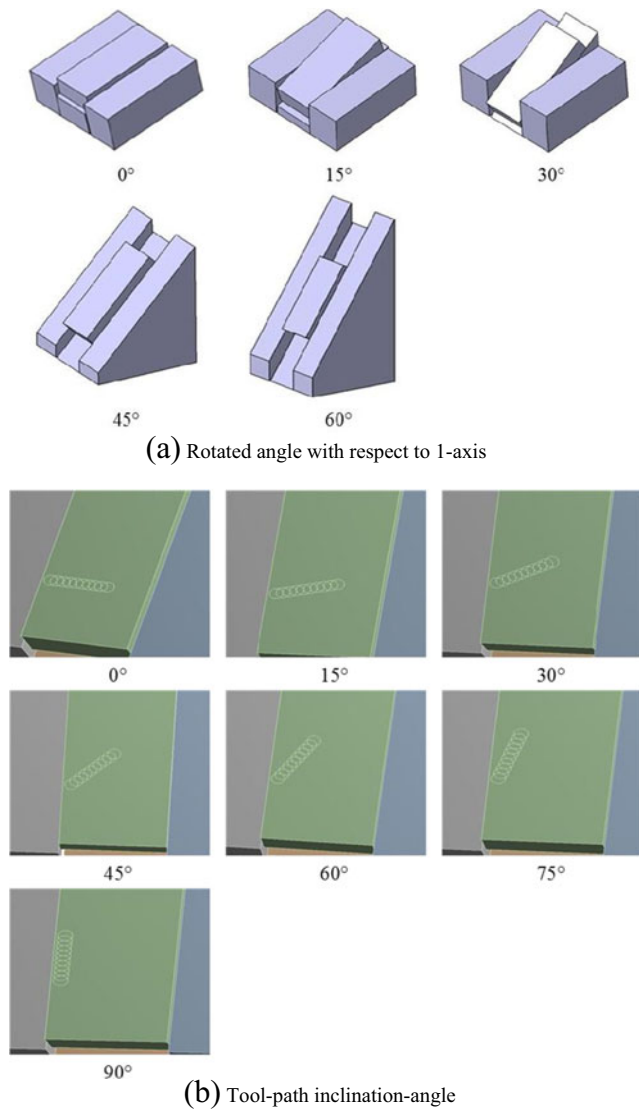


Fig. 2 **a** Rotated angle with respect to one axis and **b** tool path inclination angle of workpiece

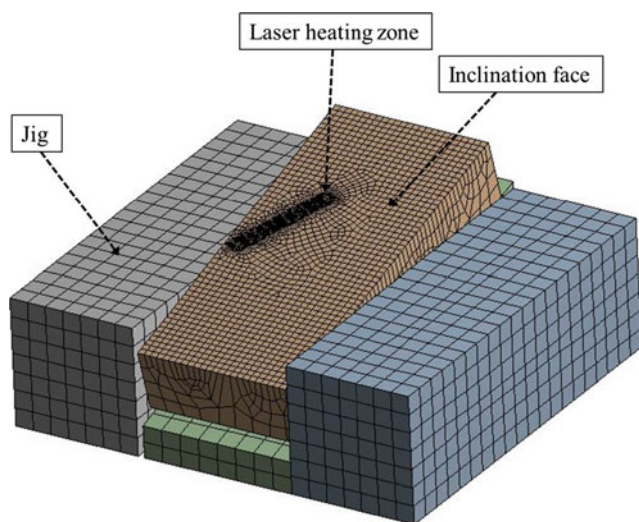


Fig. 3 Analysis model

where m , c_p , ΔT , E_L , and Δt are the weight of the workpiece, specific heat, increase of temperature, laser power, and laser irradiation time, respectively. Also, the laser absorptivity is slightly changed depending on the shape and color of the workpiece, the surface roughness, etc. Therefore, an accurate value of laser absorptivity cannot be expressed, and the laser absorptivity can be adjusted by comparing the analysis results and experiments.

First, when the laser absorptivity was applied as 0.35 in the analyses, the error rate between the thermal analyses and experiments was more than 10 % in all cases. Secondly, when the laser absorptivity was applied as 0.4, the error rate between the thermal analyses and experiments was less than 5 % in all cases. So, laser absorptivity was determined to be 0.4, and this value was applied to calculating the optimized laser power.

2.5 Analysis conditions

In LAM, the machining conditions, such as laser power, should be set to the optimum preheating range, that is, at a level that can reduce the yield strength in a workpiece [23, 27]. As the preheating range of titanium alloy is about 450–600 °C, it is important to induce this preheating temperature [28, 29]. In this study, the laser power in the thermal analysis was 80 W, and the feed rate was set to 100 mm/min. Based on the selected absorptivity of titanium alloy, 0.4, the laser power was set to 32 W [25, 26]. The details of the thermal analysis are presented in Table 1, and the thermal conductivity coefficient and specific heat capacity are presented in Table 2 [26].

2.6 Analysis results

The thermal analysis was performed according to the analysis conditions presented in Section 2.5. The results obtained by the thermal analysis with a laser output of 80 W were usually fitted to the optimal preheating temperature of the titanium alloy, 450–600 °C. The preheating temperature decreased according to increases in the tool path inclination angle, but the preheating temperature increased above the tool path inclination angle of 75°. For accurate analysis of the preheating

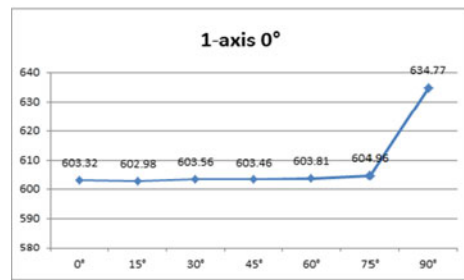
Table 1 Boundary conditions of the thermal analyses

Material	Ti-6Al-4V
Convective heat	5 W/m ²
Heat source diameter	3 mm
Laser power	80 W (32 W considering the absorptivity for the analysis)
Laser feed rate	100 mm/min
One-axis angle	0°, 15°, 30°, 45°, 60°
Tool path inclination angle	0°, 15°, 30°, 45°, 60°, 75°, 90°

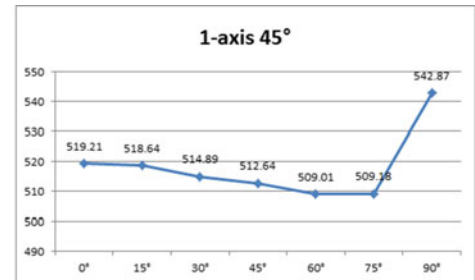
Table 2 Properties of the Ti-6Al-4V according to temperature change

Temperature (°C)	Density (kg/m ³)	Thermal conductivity (W/m K)	Specific heat (J/kg K)
25	4420	7	546
100	4406	7.45	562
200	4395	8.75	584
300	4381	10.15	606
400	4366	11.35	629
500	4350	12.6	651
600	4336	14.2	673
700	4324	15.5	694
800	4309	17.8	714
900	4294	20.2	734
995	4282	19.3	641
1100	4267	21	660
1200	4252	22.9	678
1300	4240	23.7	696
1400	4225	24.6	714
1500	4205	25.8	732
1600	4198	27	750
1650	4189	28.4	759

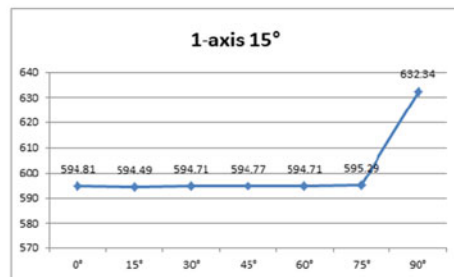
Fig. 4 Temperature distribution graph of rotated angle with respect to one axis according to tool path inclination angle. **a** One-axis angle 0°. **b** One-axis angle 15°. **c** One-axis angle 30°. **d** One-axis angle 45°. **e** One-axis angle 60°



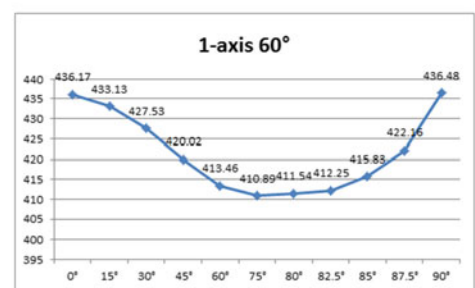
(a) 1-axis angle 0°



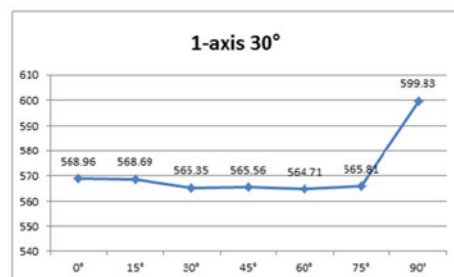
(d) 1-axis angle 45°



(b) 1-axis angle 15°



(e) 1-axis angle 60°



(c) 1-axis angle 30°

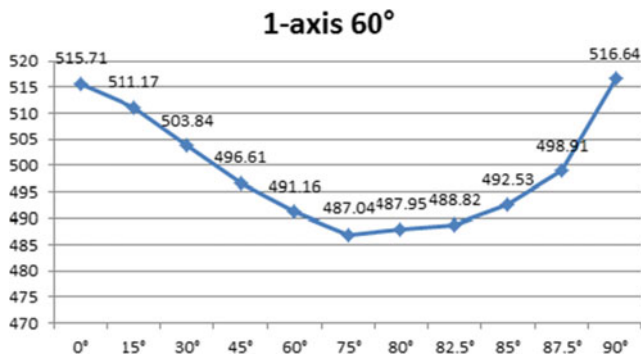


Fig. 5 Temperature distribution graph of rotated angle with respect to one-axis 60° according to tool path inclination angle

temperature, additional thermal analyses were performed for the range of 75°–90°. Figure 4 represents temperature distributions according to inclination angles including additional thermal analyses [30].

The results of the thermal analyses showed that, when the rotated angle was more than 30° with respect to one axis, the preheating temperature decreased according to increases in the tool path inclination angle, but it increased at the angle of 75°. Although most preheating temperatures were fitted to the optimal preheating temperature of titanium materials, the rotated angle of 60° with respect to one axis was not fitted to the optimal preheating temperature. Thus, an additional thermal analysis was performed with the laser power increased to 100 W (40 W considering the absorptivity for the analysis). Figure 5 shows the results of the thermal analysis.

3 Experiment

3.1 Experimental setup

The machining experiment in this study was performed using a CNC five-axis machining center, Hi-V560M by Hyundai-WIA, with a laser module, LDM-1000-100 by Laserline. Also, a pyrometer was installed at the laser module to measure the laser spot temperature of the workpiece. In the laser module, a high-power diode laser (HPDL) which had a maximum power of 1 kW and a wavelength of 808–980 nm was used. A dynamometer (9257B by Kistler) and a charge amplifier (5019 by Kistler) were also used to measure the cutting force.

Table 3 Instruments and specifications

Instrument	Company	Specification
Machining center	Hyundai-WIA	Hi-V560M
Laser optic module	Laserline	LDM 1000-100
Dynamometer	Kistler	9257B
Charge amplifier	Kistler	5019

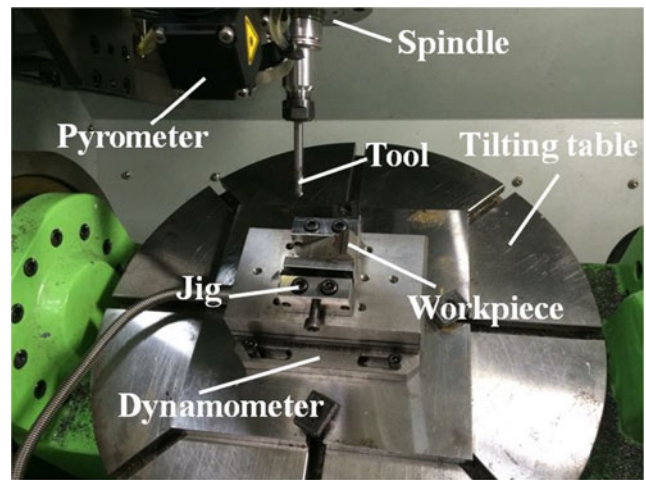


Fig. 6 Experimental setup for laser-assisted machining

Table 3 shows the equipment used in this experiment, and Fig. 6 shows the established LAM system [23].

3.2 Experimental conditions

Table 4 presents the experimental conditions in this machining experiment. The rotation speed, the feed rate, and the depth of cut of the main axis were 3000 rpm, 100 mm/min, and 0.5 mm, respectively. For the rotated angle with respect to one axis, three angles of 30°, 45°, and 60° were selected, and tool path inclination angles of 0°, 30°, 60°, and 90° were selected. A total of 12 machining experiments were performed. The laser power used in the LAM was 80 W. In the case of the rotated angle with respect to one axis for 60°, the laser power used was 100 W.

4 Results and discussion

4.1 Comparison of the analysis and preheating experiment

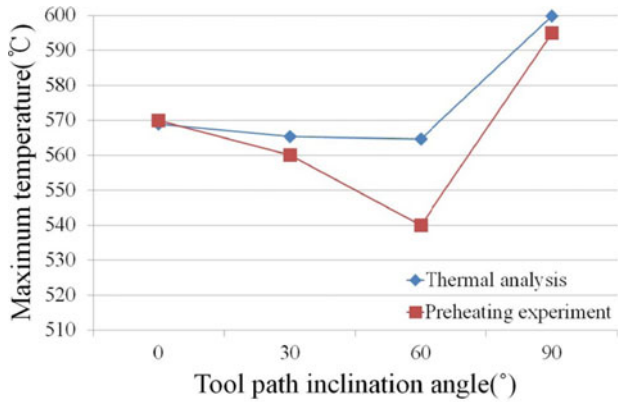
A preheating experiment was performed on the titanium alloy before the machining experiment was carried out based on the laser output estimated in the thermal analysis presented in Section 2.6. The temperature of the laser heat source was measured using a pyrometer, and the results of the preheating experiment in this section and the results of the thermal

Table 4 Conditions of the experiment

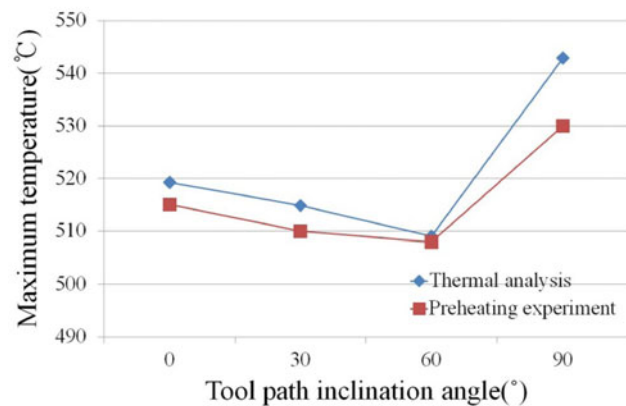
Material	Ti-6Al-4V
Laser power	80, 100 W
Feed rate	100 mm/min
Rotational speed	3000 rpm
Depth of cut	0.5 mm
Block size	55×25×11 mm
Laser heat source size	3Ø

analysis performed in Section 2.6 were compared and analyzed. Figure 7 and Table 5 compare the results of the preheating experiment and those of the thermal analysis.

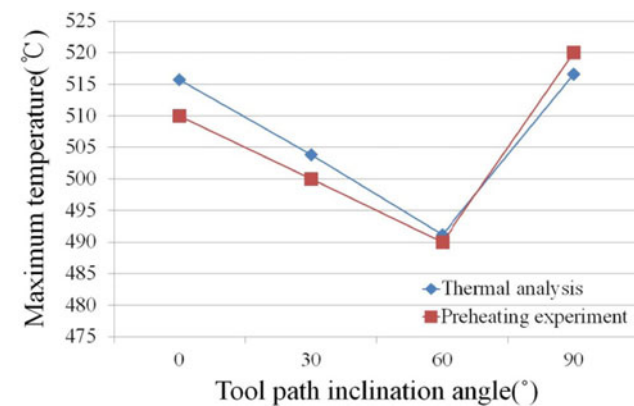
In the comparison of the maximum temperature obtained from the preheating experiment and the thermal analysis, the error ranged from 0.21 to 4.34 %. The error in the rotated



(a) 1-axis angle 30°



(b) 1-axis angle 45°



(c) 1-axis angle 60°

Fig. 7 Comparison of temperature distributions of the workpiece between thermal analysis and experiment according to angle. **a** One-axis angle 30°. **b** One-axis angle 45°. **c** One-axis angle 60°

Table 5 Comparison of maximum temperature of the workpiece between thermal analysis and experiment according to angle

Rotated angle with respect to one axis (°)	Tool path inclination angle (°)	Thermal analysis temperature (°C)	Preheating experiment temperature (°C)	Error (%)
30	0	568.9	570.9	0.35
	30	565.3	560.1	0.92
	60	564.7	540.2	4.34
	90	599.8	595.2	0.77
45	0	519.2	515.1	0.79
	30	514.8	510.2	0.89
	60	509.1	508.2	0.18
	90	542.8	530.3	2.31
60	0	515.7	510.2	1.07
	30	503.8	500.1	0.73
	60	491.1	490.1	0.21
	90	516.6	520.8	0.81

angle with respect to one axis for 30° showed the largest value of 4.34 % at the tool path inclination angle of 60°. Most cases showed very small error, and the results obtained in the preheating experiment and the thermal analysis were almost the same.

4.2 Machining experiment

In the case of the rotated angles of 30° and 45° with respect to one axis, the applied laser power was 80 W, and the power of 100 W was applied to the angle of 60°. As shown in Table 4, the rotation speed, the feed rate, and the depth of cut of the main axis were 3,000 rpm, 100 mm/min, and 0.5 mm, respectively. Figure 8 shows an image of the machined workpiece, and Table 6 shows the measurement results of the cutting force. The cutting force decreased according to the increase

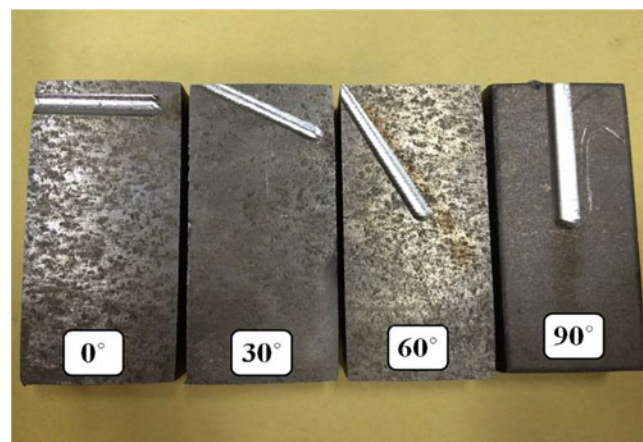


Fig. 8 The machined surface of Ti-6Al-4V by applying tool path inclination angle

Table 6 Measured cutting force

One-axis 30°		One-axis 45°		One-axis 60°	
Degree (°)	Cutting force (N)	Degree (°)	Cutting force (N)	Degree (°)	Cutting force (N)
0	20	0	7	0	6
30	11	30	5	30	8
60	3	60	4	60	7
90	5	90	8	90	4

in the tool path inclination angle regardless of the rotated angle with respect to one axis, because the workpiece was machined at the edge of the tool [23].

5 Conclusions

In this work, optimization of preheating and machining based on tool path inclination angle was studied.

1. Thermal analysis of a titanium alloy was performed by finite element analysis. Based on the analysis, the optimal laser power was calculated for the LAM of a titanium alloy workpiece according to the tool path inclination angle.
2. It was shown that the preheating temperature decreased according to increases in the tool path inclination angle, but the preheating temperature increased when the tool path inclination angle was 75° or more.
3. In the preheating experiment with the same conditions as those of the thermal analysis, the error ranged from 0.21 to 4.34 % in relation to the laser power, and the maximum error was 4.34 % at the rotated angle with respect to one axis for 30° with the tool path inclination angle of 60°. Most cases showed very small error, and the results obtained in the preheating experiment and the thermal analysis were almost the same.
4. In the case of rotated angles of 30° and 45° with respect to one axis, the applied laser power was 80 W, and the power of 100 W was applied to the angle of 60°. The cutting force decreased according to the increase in the tool path inclination angle regardless of the rotated angle with respect to one axis.

It is expected that the results obtained in this study can be used as reference data for estimating preheating temperatures and machinabilities in machining experiments with various flat materials.

Acknowledgments This research was supported by the Basic Science Research Program through the National Research Foundation of Korea funded by the Ministry of Science, ICT & Future Planning (No. 2014022060).

References

1. Lee JH, Shin DS, Suh J, Cho HY, Kim KW (2008) Trends of laser integrated machine. *J Korean Soc Precis Eng* 25:20–26
2. Pei ZJ, Khanna N, Ferreira PM (1995) Rotary ultrasonic machining of structural ceramics—a review. *Ceram Eng Sci Proc* 16:259–278
3. Chang CW, Kuo CP (2007) An investigation of laser-assisted machining of Al₂O₃ ceramics planning. *Int J Mach Tools Manuf* 47: 452–461
4. Research report of the National Research Foundation of Korea (NRF) (2014) A new conceptual 3-dimensional laser assisted machining system 2013035186
5. Melkote S, Kumar M, Hashimoto F, Lahoti G (2009) Laser assisted micro-milling of hard-to-machine materials. *J CIRP* 58:45–48
6. Ding H, Shin YC (2010) Laser-assisted machining of hardened steel parts with surface integrity analysis. *Int J Mach Tools Manuf* 50:106–114
7. Brecher C, Emonts M, Rosen CJ, Hermani JP (2011) Laser-assisted milling of advanced materials. *Phys Procedia* 12:599–606
8. Zhang X, Liu CR, Yao Z (2007) Experimental study and evaluation methodology on hard surface integrity. *Int J Adv Manuf Technol* 34:141–148
9. Chang CW, Kuo CP (2007) An investigation of laser-assisted machining of Al₂O₃ ceramics planning. *Int J Mach Tools Manuf* 47: 452–461
10. Kim KS, Lee CM (2011) Analysis of moving heat source for laser assisted machining of plate by feed rate control. *J Korean Soc Precis Eng* 28:1341–1346
11. Lee SJ, Kim JD, Suh J (2014) Microstructural variations machining characteristics of silicon nitride ceramics from increasing the temperature in laser assisted machining. *Int J Precis Eng Manuf* 15: 1269–1274
12. Pfefferkorn FE, Incropera FP, Shin YC (2005) Heat transfer model of semi-transparent ceramics undergoing laser-assisted machining. *Int J Heat Mass Transf* 48:1999–2012
13. Ding H, Shen N, Shin YC (2012) Thermal and mechanical modeling analysis of laser-assisted micro-milling of difficult-to-machine alloys. *J Mater Process Technol* 212:601–613
14. Kalyon M, Yilbas BS (2003) Laser pulse heating: a formulation of desired temperature at the surface. *Opt Lasers Eng* 39:109–119
15. Yang B, Shen X, Lei S (2009) Mechanisms of edge chipping in laser-assisted milling of silicon. *Int J Mach Tools Manuf* 49:344–350
16. Kim JH, Choi JY, Lee CM (2014) A study on the effect of laser preheating on laser assisted turn-mill for machining square and spline members. *Int J Precis Eng Manuf* 15:275–282
17. Kim TW, Lee CM (2015) Determination of the machining parameters of nickel-based alloys by high-power diode laser. *Int J Precis Eng Manuf* 16:309–314
18. Rozzi JC, Pfefferkorn FE, Shin YC (2000) Experimental evaluation of the laser assisted machining of silicon nitride ceramics. *J Manuf Sci Eng* 122:666–670
19. Kim DH, Lee CM (2014) A study of cutting force and preheating-temperature prediction for laser-assisted milling of Inconel 718 and AISI 1045 steel. *Int J Heat Mass Transf* 71:264–274
20. Kang DW, Lee CM (2014) A study on the development of the laser-assisted milling process and a related constitutive equation for silicon nitride. *CIRP Ann Manuf Technol* 63:109–112
21. Kang DW, Lee CM (2013) A study on determining the exponents for a constitutive equation in laser assisted machining. *Int J Precis Eng Manuf* 14:2051–2054
22. Lei S, Shin YC, Incropera FP (2000) Deformation mechanisms and constitutive modeling for silicon nitride undergoing laser-assisted machining. *Int J Mach Tools Manuf* 40:2213–2233

23. Sim MS (2015) A study on laser assisted machining according to tool path Inclination angle of inclined workpiece and workpiece with rotated angle with respect to 2-axis. Dissertation of Changwon National University, Republic of Korea M. S
24. Kim KS, Lee CM (2012) Prediction of preheating conditions for the inclined laser assisted machining. *J Cent South Univ* 19:3079–3083
25. Kim DH and Lee CM (2013) A fundamental study on the absorptivity of diode laser for titanium alloy. Proc. of the KSMTE Spring conference 235
26. Yang J, Sun S, Brandt M, Yan W (2010) Experimental investigation and 3D finite element prediction of the heat affected zone during laser assisted machining of Ti6Al4V alloy. *J Mater Process Technol* 210:2215–2222
27. Neugebauer R, Denkena B, Wegener K (2007) Mechatronic systems for machine tools. *CIRP Ann Manuf Technol* 56:657–686
28. Brecher C, Rosen CJ, Emonts M (2010) Laser-assisted milling of advanced materials. *Phys Procedia* 5:259–272
29. Kim TW, Lee CM (2015) A study on the development of milling process for silicon nitride using ball end-mill tools by laser-assisted machining. *Int J Adv Manuf Technol* 77:1205–1211
30. Sim MS, Lee CM (2014) A study on the laser preheating effect of Inconel 718 specimen with rotated angle with respect to 2-axis. *Int J Precis Eng Manuf* 15:189–192